

See discussions, stats, and author profiles for this publication at: <https://www.researchgate.net/publication/348338637>

# The Complexity of Microbial Metal Nanoparticle Synthesis: A Study of *Candida parapsilosis* ATCC 7330 mediated Gold Nanoparticles Formation

Article in *BioNanoScience* · June 2021

DOI: 10.1007/s12668-021-00825-6

CITATIONS

3

READS

185

4 authors:



Saravanan Krishnan

41 PUBLICATIONS 270 CITATIONS

SEE PROFILE



Deepthy Jayakumar

University of Madras

8 PUBLICATIONS 72 CITATIONS

SEE PROFILE



Harishkumar Madhyastha

Miyazaki University

166 PUBLICATIONS 2,200 CITATIONS

SEE PROFILE



Anju Chadha

Indian Institute of Technology Madras

166 PUBLICATIONS 3,495 CITATIONS

SEE PROFILE



# The Complexity of Microbial Metal Nanoparticle Synthesis: A Study of *Candida parapsilosis* ATCC 7330 mediated Gold Nanoparticles Formation

Saravanan Krishnan<sup>1</sup> · Deepthy Jayakumar<sup>1</sup> · Harishkumar Madhyastha<sup>2</sup> · Anju Chadha<sup>1,3</sup>

Accepted: 7 January 2021

© The Author(s), under exclusive licence to Springer Science+Business Media, LLC part of Springer Nature 2021

## Abstract

Understanding the biosynthetic mechanism of gold nanoparticle formation is the key to controlling the size, dispersity, and morphology of the nanoparticles. Reduction of gold (III) to gold (0) in cell-free extracts of *Candida parapsilosis* ATCC 7330 is not only enzymatic, as confirmed by experiments with heat denatured extracts. In addition to proteins, cellular reducing equivalents also contribute to the formation of gold nanoparticles in a concentration-dependent manner. Characterization of the bio-synthesized gold nanoparticles using X-ray photoelectron spectroscopy and elemental analysis revealed that nanoparticles are stabilized by proteins. The importance of protein three-dimensional structure in producing stable gold nanoparticles is also addressed. Making free thiol groups (–SH) unavailable by derivatizing them in protein extracts resulted in monodisperse gold nanoparticles implying that free –SH increase aggregation and emphasize this as a possible strategy to produce monodisperse gold nanoparticles in biological extracts which is otherwise difficult.

**Keywords** Gold nanoparticles · Biosynthesis · Mechanism · Reduction · Stabilization · Proteins

## 1 Introduction

Bio-inspired syntheses of metal nanoparticles are feasible, environmentally benign [1], and meet most of the design principles under green chemistry [2]. Among the bio-inspired methods, microbial synthesis of nanoparticles, especially gold, is widely reported [3, 4]. Gold nanoparticles are widely used in various applications in biomedicine and catalysis even though different microbes, namely bacteria, fungi, actinomycetes, and algae, have been reported for the synthesis of gold (Au) nanoparticles (NPs). The most preferred are the fungal species for the synthesis of Au NPs due to advantages such as high metal tolerance [5], ease of handling, scale-up procedures, presence of redox enzymes, and capping agents [6]. In order to gain control over the size, shape, and dispersity

of the nanoparticles formed, it is imperative to understand the mechanism of bio-synthesis of gold nanoparticles mediated by micro-organism.

Several fungi have been reported for the synthesis of Au NPs [7] but the mechanism of formation of nanoparticles is not completely understood. Most of the reports have only speculated that the reduction of gold (III) ions to gold (0) atoms is mediated by enzymes. Two different routes reported for the bioreduction of gold (III) using the fungus *Botrytis cinerea* were established—(i) nicotinamide adenine dinucleotide (NADH)–dependent reductases for the enzymatic reduction and (ii) the non-enzymatic reduction by heat stable molecules, to synthesize Au NPs of various shapes with sizes ranging from 1 to 100 nm [8]. In the yeast *Yarrowia lipolytica*, Au NPs are formed involving functional groups such as carboxyl, hydroxyl, and amide groups present on the cell surface [9]. Bioreductants such as NADH produced by the fermentation of lactate in the yeast, *Hansenula anomala*, also reportedly synthesize Au NPs (size: 14 nm) [10]. Besides, the synthesis of gold nanoparticles using *Candida* sp. [11–13] is also established but biosynthetic mechanism is not reported so far.

Stabilization of the reduced gold nanoparticles is the most important step to prevent the formation of particle aggregates. Generally, capping molecules involved in stabilization of nanoparticles are analyzed using FT-IR spectroscopy [14].

✉ Anju Chadha  
anjuc@iitm.ac.in; anjuchadha55@gmail.com

<sup>1</sup> Laboratory of Bio-organic Chemistry, Department of Biotechnology, Indian Institute of Technology Madras, Chennai 600036, India

<sup>2</sup> Department of Applied Physiology, Faculty of Medicine, University of Miyazaki, Miyazaki, Japan

<sup>3</sup> National Centre for Catalysis Research, Indian Institute of Technology Madras, Chennai 600036, India

For example, phosphate groups and polypeptides/proteins were detected in the Au NPs formed by *R. oryzae* biomass [15]. The nature of stabilizers and their binding to gold nanoparticles is yet to be understood completely.

*Candida parapsilosis* ATCC 7330, a versatile biocatalyst largely studied for enzyme-mediated biotransformation reactions [16], has been recently used for the synthesis of colloidal Au NPs [17]. However, the mechanism of formation of the gold nanoparticles using *Candida parapsilosis* ATCC 7330 is not established as yet. The present study addresses the mechanistic aspects of gold nanoparticle formation, i.e., bioreduction and stabilization of Au NPs, in cell-free extracts of *Candida parapsilosis* ATCC 7330. The multiple ways by which reduction of gold (III) to gold (0) can occur and also the details of the stabilization of the gold (0) have resulted in investigating the role of native protein conformation and the influence of free protein thiols (-SH) in the biogenesis of Au NPs using yeast cell extracts.

## 2 Experimental

### 2.1 Biosynthesis of Gold Nanoparticles (Au NPs) Using *Candida parapsilosis* ATCC 7330

Colloidal gold nanoparticles is prepared using the cell-free extracts of *Candida parapsilosis* ATCC 7330 strain (ATCC, Manassas, VA 20108, USA) using the reported procedure [17]. Reactions of Au NPs synthesis were carried out using MilliQ water and conical flasks were washed with *aqua regia* before use. Protein concentration in the cell-free extract was estimated using Bradford reagent (Sigma-Aldrich).

### 2.2 Synthesis of Au NPs Using NADH, GSH, Ascorbic Acid, and Glucose

NADH, a redox cofactor, was tested for the synthesis of Au NPs by titrating against 1 mM of gold (III) for the concentrations ranging from 0.2  $\mu\text{M}$  to 3 mM. Similarly, varying concentration ( $10^{-6}$  M –  $4 \times 10^{-3}$  M) of glutathione was tested against 1 mM gold (III) chloride for the synthesis of Au NPs. Titration of either ascorbic acid (0.1–0.5 mM) or glucose (0.1–0.5 mM) against the fixed amount of AuCl<sub>3</sub> solution (1 mM) was carried out. For these experiments, the final volume of the reaction mixture was adjusted with phosphate buffer (pH 7.0, 20 mM) and the reaction flasks were incubated in orbital shaker for 72 h, 200 rpm at 37 °C.

### 2.3 Estimation of Reducing Activity

For cell-free extract, heat-denatured extract, and bioreductants, the reducing activity was assayed using standard protocol [18]. Calibration curve was plotted using a known reducing agent,

ascorbic acid (5–25  $\mu\text{g}/\text{mL}$ ). To the test sample, 0.5 mL of 0.02 M sodium phosphate buffer was added and 1% w/v aqueous potassium ferrocyanide (0.5 mL) was added later. This mixture was incubated at 50 °C for 20 min and then cooled rapidly, followed by addition of 0.5 mL of 10% w/v trichloroacetic acid and centrifugation at 3000 $\times$ g for 10 min. The supernatant (1.5 mL) was collected; 0.2 mL of 0.1% FeCl<sub>3</sub> was added to it. Absorbance at 700 nm (visible range) against the blank was recorded using a UV/Vis spectrophotometer.

### 2.4 BSA-Mediated Preparation of Au NPs

Bovine serum albumin (BSA) of different concentrations (0.72–21.6  $\mu\text{M}$ ) were titrated against 1 mM AuCl<sub>3</sub> solution for the preparation of Au NPs. The reaction with heat-denatured BSA (microwave oven (700 W, 2 min)) was also carried out.

In an identical study, the effect of protein conformation on the synthesis of colloidal Au NPs was studied by the addition of native BSA to denatured cell-free extract. For this experiment, varying BSA concentrations (2.2–4.32  $\mu\text{M}$ ) were added to an identical reaction flask comprising of either cell-free extract or heat-denatured extract. Reaction with cell-free extract and heat-treated extract alone are kept as control experiments. In reaction flasks, AuCl<sub>3</sub> was added to make overall 1 mM concentration and the flasks were incubated in orbital shaker for 72 h, 200 rpm at 37 °C.

### 2.5 Kinetics Study of Au NP Formation

For any processes like biosynthesis of metal nanoparticles, kinetic study is imperative to understand the dynamics of the reaction. For this, gold (III) chloride was added to make overall concentration of 1 mM either with cell-free extract or heat-denatured extract. Reaction flasks were incubated in an orbital shaker at 37 °C, 200 rpm. Samples were collected at different time intervals during 72 h incubation time.

### 2.6 Stability of Au NPs in the Presence of Thiol Ligands

It is important to understand the stability of Au NPs in the presence of thiol-containing stabilizer like cysteine. For this, cysteine was added to make overall concentration of 0–100  $\mu\text{M}$  with 0.5 mL of Au NPs. Gold nanoparticles used in this study were prepared using the Turkevich method [19]. Samples were incubated at 25 °C for 24 h.

### 2.7 Estimation of the Total Thiol Content in the Cell-Free Extract

Total thiol content in the cell-free extract was estimated using Ellman's reagent, 5, 5'-dithio-bis-(2-nitrobenzoic

acid) (DTNB) [20]. To 0.5 mL of the cell-free extract, 0.6 mL of the DTNB (0.25 mM prepared in methanol) was added and the total volume made up to 1.5 mL using methanol. The mixture was incubated for 15 min and then centrifuged at  $3000\times g$  for 15 min. Absorbance was recorded for the supernatant sample at 412 nm using a UV/Vis spectrophotometer. Acetyl cysteine (31–1000  $\mu\text{M}$ ) was used as standard to prepare calibration curve.

## 2.8 Influence of Free Protein Thiol Groups on Biosynthesis of Au NPs

The role of free protein thiols in the biosynthesis of Au NPs was studied by performing experiments using the thiol-modified protein extract. A stock solution of 5.6 mM *p*-Chloro mercuric benzoate (pCMB) was prepared in 0.05 N NaOH, used to derivatize the cellular thiol residues. After addition of the equivalent amounts of thiol modifiers, the reaction flasks were incubated at 25 °C, 150 rpm for overnight. Consecutively, gold precursor was added to the thiol-modified extracts to make an overall concentration of 1 mM. Reaction flasks were allowed to incubate for 72 h, 200 rpm at 37 °C. In another set of studies, after thiol modification of the protein extract, ascorbic acid (0.2 mM) was added then, and gold (III) precursor of 1 mM concentration was added to the same flasks. The reaction flasks were kept for orbital shaking for 24 h at 200 rpm, 37 °C.

## 2.9 Instruments and Characterization Techniques

Surface plasmon resonance (SPR) peak ( $\sim 520\text{--}580\text{ nm}$ ) of the Au NPs was monitored using JASCO V-530 UV/Vis spectrophotometer. Average size and polydispersity index (PDI) of Au NPs were determined using Zetasizer 3000 HSA (MALVERN Instruments) and nanoparticle analyzer SZ-100 (HORIBA Scientific nanoPartica). For colloidal Au NPs, a drop of the sample was casted on carbon-coated copper grids, air dried and taken for further analysis using the PHILIPS CM12 transmission electron microscope.

The concentration of Au NPs in the colloidal solution was measured using ICP-OES analysis (PERKIN ELMER Optima 5300 DV) after acid digestion of the nanoparticle pellet. X-ray photoelectron spectroscopy analysis of freeze-dried pellet of biosynthesized Au NPs was recorded using AXIS-HS (SHIMADZU-Kratos.Co) with Mg  $K\alpha$  radiation source (15 keV). Elemental analysis of the freeze-dried pellet of biosynthesized Au NPs was determined with the help of a CHN analyzer (PERKIN ELMER 2400 Series).

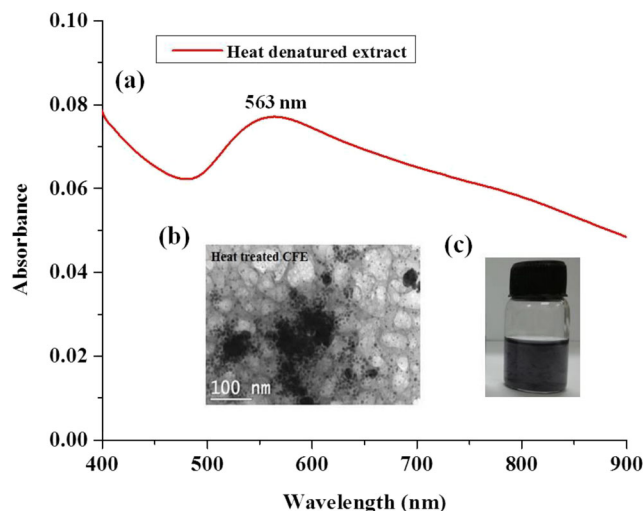


**Fig. 1** Biosynthesis of gold nanoparticles using heat-denatured extract (red line) of *Candida parapsilosis* ATCC 7330. **a** UV/Vis spectra, **b** transmission electron micrographs, and **(c)** visual inspection

## 3 Results and Discussion

### 3.1 Investigation on Bioreduction of Gold (III) as the First Step of NP Formation

Our earlier study showed that Au NPs of hydrodynamic diameter  $59.2 \pm 1\text{ nm}$  were formed in cell-free extracts of 24 h grown *Candida parapsilosis* ATCC 7330 which depends on total cellular protein concentration and not only the enzymatic activity of reductase [17]. Among the different culture ages (12, 24, 36, and 48 h) investigated, cell-free extract prepared from 24 h grown yeast cells was found optimum for the biosynthesis of gold nanoparticles based on nanoparticles attributes (Figs. S1 and S2; Tables S1 and S2). Experiments with heat-denatured cell-free extracts (no reductase activity) resulted in the formation of gold particle aggregates ( $\sim 48\%$  yield), as seen by surface plasmon

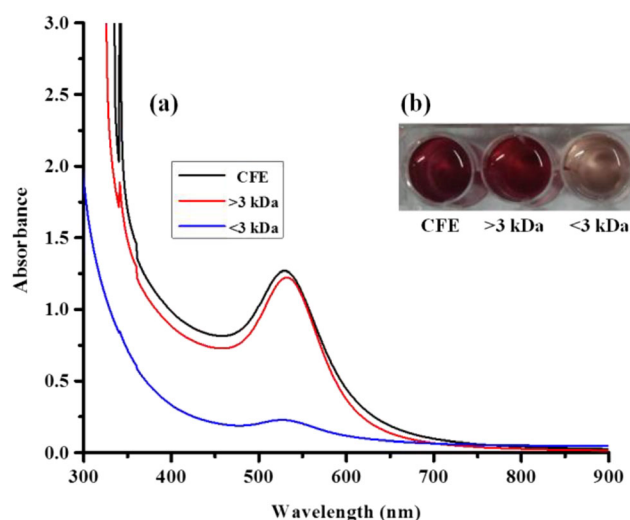


**Fig. 2** Biosynthesis of gold nanoparticles using the cell-free extract,  $> 3\text{ kDa}$  and  $< 3\text{ kDa}$  fractions. **a** UV/Vis spectra and **b** visual inspection

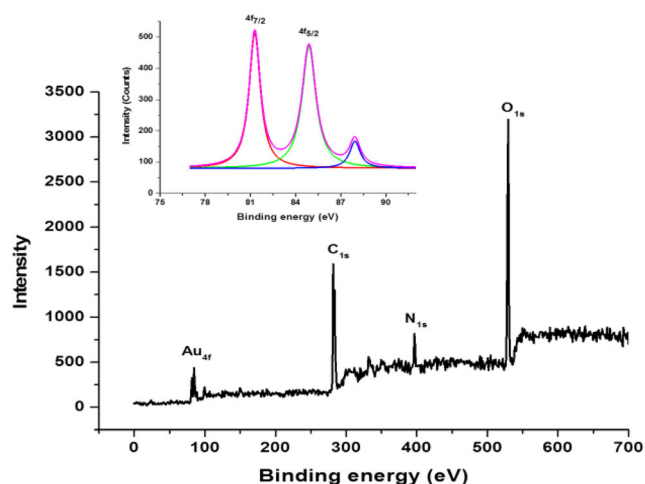


**Fig. 3** Wide scan X-ray photoelectron spectroscopy of the gold nanoparticles prepared by cell-free extract and the inset shows the XPS of Au (4f)

resonance (SPR) wavelength maxima ( $\lambda_{\max}$ ) of 563 nm (Fig. 1) suggesting that the reduction of gold (III) in cell-free extracts is not purely enzymatic, contrary to reports so far which state that the reduction of gold (III) is enzymatic and depends on reductases and/or other cellular enzymes in cell-free extracts [21–26].

Estimation of the reducibility of metal ions such as gold (III) by the native cell-free extract and heat-denatured cell-free extract was carried out using an  $\text{Fe}^{3+}$ -based assay [27] (Fig. S3). The higher the redox potential, the better is the reducibility of the metal ions by the reducing agent. Redox potential of aqueous  $\text{Fe}^{3+}$  (0.77 eV) is nearly half of the aqueous solution of gold (III) ions (1.4 eV) [28]. Compared to the cell-free extract, only 28% residual reducing activity was observed with the heat-denatured extract. In other words, 72% reducing

**Table 1** Effect of BSA addition to the heat-denatured extract used for the synthesis of gold nanoparticles (Au NPs)

| BSA added to the denatured extract ( $\mu\text{M}$ ) | SPR Wavelength maxima (nm) of Au NPs | Hydrodynamic diameter (nm) of Au NPs | Polydispersity index (PDI) of Au NPs |
|--|--------------------------------------|--------------------------------------|--------------------------------------|
| Control  | 541                                  | $93.87 \pm 1.42$                     | $0.36 \pm 0.05$                      |
| 2.16   | 539                                  | $71.97 \pm 0.59$                     | $0.36 \pm 0.01$                      |
| 2.88   | 539                                  | $71.86 \pm 0.47$                     | $0.36 \pm 0.02$                      |
| 3.76   | 541                                  | $71.83 \pm 0.98$                     | $0.36 \pm 0.01$                      |
| 4.32   | 536                                  | $70.14 \pm 1.67$                     | $0.35 \pm 0.02$                      |

activity was lost due to heat treatment of the cell-free extract. Clearly, this study indicates that heat stable bioreductants present in the denatured cell-free extract also contribute to the reduction of gold (III) to gold (0).

A typical yeast cell comprises 40–55% proteins, 20–35% polysaccharides, 7–15% lipids, 6–12% RNA, and 1–3% DNA [29]. Besides cellular macromolecules, small molecules such as cofactors, amino acids, sugars, and organic acids are present inside the fungi, which might also mediate the reduction of gold (III). Nicotinamide adenine dinucleotide (NADH), glutathione (GSH), ascorbic acid, and glucose were used as bioreductants to reduce  $\text{AuCl}_3$ . Systematic studies revealed the following observations: (1) Reduction of gold (III) to gold (0) mediated by bioreductants is concentration dependent and (2) not all reductants reduce gold (III) and produce gold nanoparticles. In case of NADH, surface plasmon resonance (SPR) corresponding to Au NP ( $3.8 \text{ nm} \pm 0.5 \text{ nm}$ ) formation increases with the increase in NADH up to 3 mM, which was in consensus with the nanofabrication process (Figs. S4 and S5). Titration experiments

**Fig. 4** Biosynthesis of gold nanoparticles using ascorbic acid (0.2 mM) and > 3 kDa fraction of cell-free extract of varying protein concentration (0–600  $\mu\text{g}/\text{mL}$ ). **a** UV/Vis spectra and **b** visual inspection

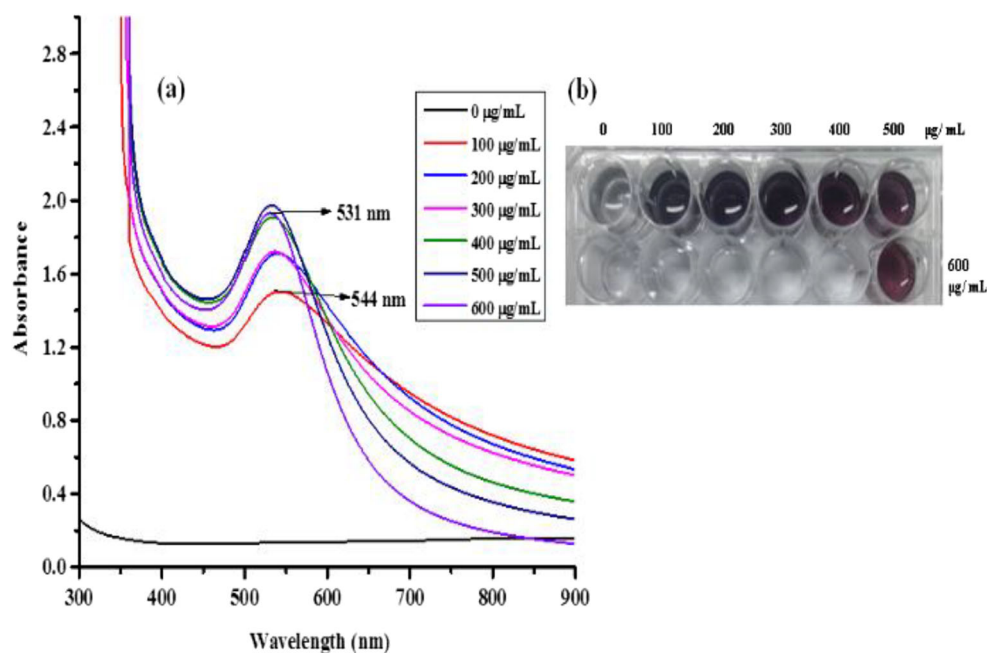
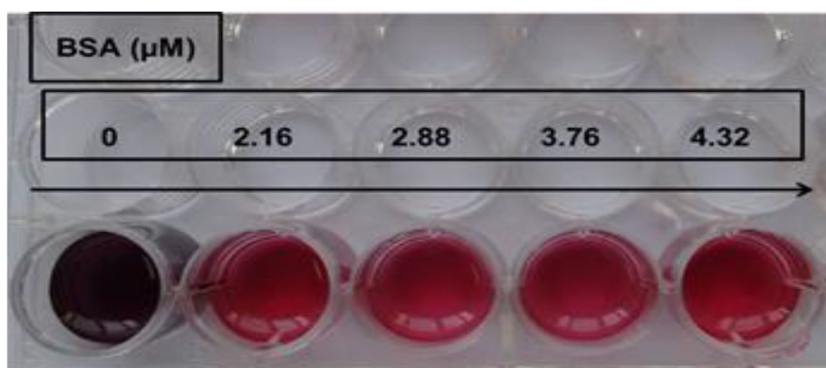




**Fig. 5** Visual representation of the synthesis of gold nanoparticles using heat-denatured cell-free extract with varying concentration of BSA



with glutathione, a tripeptide ( $\gamma$ -glutamylcysteinyl glycine), showed an increase in Au NP formation until 0.5 mM GSH against 1 mM  $\text{AuCl}_3$  (Fig. S6). Gold nanoparticles of mean particle size of  $25 \pm 3$  nm were formed with 0.5 mM glutathione (Fig. S7). Titration studies of ascorbic acid (0.1–0.5 mM) against  $\text{AuCl}_3$  did not show the visible formation of colloidal Au NPs (Fig. S8). Similarly, titration experiments with glucose in concentrations ranging from 0.1 to 0.5 mM did not yield colloidal Au NPs which was also consistent with visual inspection (Fig. S9). Collectively, Au NPs observed in the experiments with reducing equivalents NADH and GSH confirmed the non-enzymatic bioreduction of gold (III) to gold (0). Analysis of the reducing capacity of these bioreductants revealed that 1 mM of NADH showed reducing activity of 224  $\mu\text{g}/\text{mL}$  and GSH (1 mM) has a reducing activity of 156  $\mu\text{g}/\text{mL}$ . Very few reports indicate that the microbial reduction of gold (III) to gold (0) could be non-enzymatic [30, 31], and if they do, conclusive experimental proof is often missing.

To understand the role of proteins and the cellular bioreductants in Au NP's biosynthesis, the cell-free extract was subjected to fractionation using 3 kDa centrifugal filters. The > 3 kDa fraction rich in protein ( $\sim 831$   $\mu\text{g}/\text{mL}$ ) showed the formation of Au NPs with maximum intensity as compared to the reaction with < 3 kDa fraction where protein concentration is very low ( $\sim 13$   $\mu\text{g}/\text{mL}$ ) (Fig. 2). Remarkably,  $\text{Fe}^{3+}$ -reducing activity in > 3 kDa fraction was high (85%) and the remaining activity was retained in the < 3 kDa fraction.

### 3.2 Investigation on the Stabilization Aspects of the Formed Au NPs

Particle stabilization is very important to prevent nanoparticle aggregation [32]. Nanoparticles are mainly stabilized by electrostatic interactions and steric forces or a combination of both [33]. Elemental analysis of synthesized Au NPs showed the presence of carbon (21.23%), hydrogen (2.14%), and nitrogen (3.58%). X-ray photoelectron spectroscopic (XPS) analysis indicated the presence of gold, carbon, nitrogen, and oxygen in the lyophilized sample of biosynthesized Au NPs as per

standard values [34–37] (Fig. 3). The  $\text{Au}_{4f}$  spectrum was resolved into three peaks with binding energies of 81.2 eV and 84.8 eV which corresponds to the  $4f_{7/2}$  and  $4f_{5/2}$  levels of gold (0) and a third peak at 87.9 eV corresponds to gold (III) (Fig. S10a). The  $\text{C}_{1s}$  spectrum of the Au NPs showed two peaks with binding energies of 281.8 eV and 282.2 eV which could be assigned to C-C and C-H respectively (Fig. S10b). The  $\text{N}_{1s}$  spectrum revealed a peak with a binding energy of 396.7 eV (Fig. S10c). The strongest peak with a binding energy of 529.4 eV was identified for the surface-like oxide in the  $\text{O}_{1s}$  spectra (Fig. S10d). All these results suggest that the peptides/proteins corona formed on the nanoparticles surface as per Vroman's effect [38] could be the primary stabilizing forces. Few reports have suggested the role of proteins in nanoparticle stabilization [39]; however, the exact picture is not clear.

To study the stability exerted by proteins, synthesis of Au NPs was carried out using ascorbic acid with increasing concentrations of protein rich extract (> 3 kDa protein). As results show, the increase in protein concentration facilitated the formation of smaller size Au NPs as indicated by blue shift in

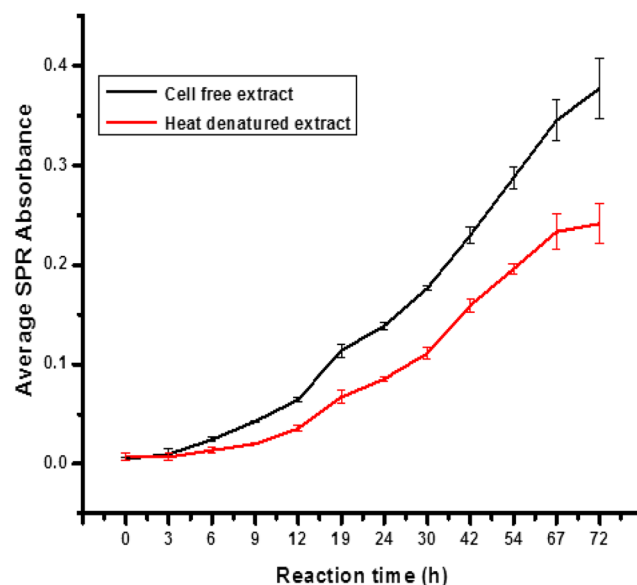
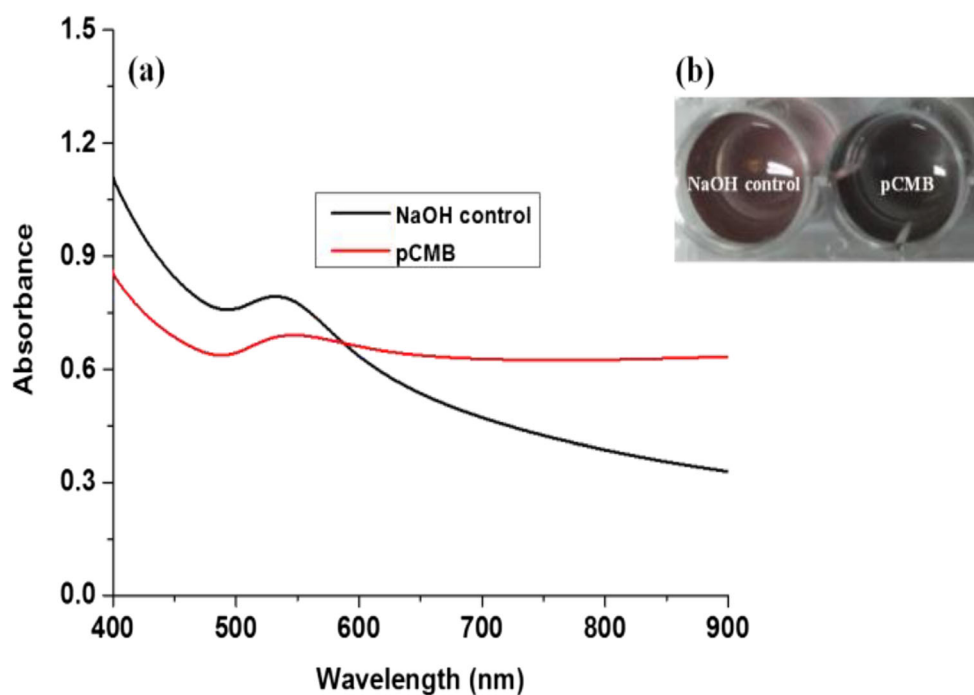


**Fig. 6** Kinetics of formation of gold nanoparticles using the cell-free extract and heat-denatured extract of *Candida parapsilosis* ATCC 7330

**Fig. 7** Synthesis of Au NPs using the thiol-modified > 3 kDa protein fraction of cell-free extract. **a** UV/Vis spectra and **b** visual inspection



SPR peak ( $\lambda_{544\text{nm}} \sim 68 \text{ nm}$  to  $\lambda_{531 \text{ nm}} \sim 42 \text{ nm}$ ) (Fig. 4) emphasizing that native proteins in the cell-free extract contribute to stabilizing the nanoparticles.

### 3.3 Effect of Protein Structure on Stability of Au NPs

The next obvious question was does the 3D structure of the protein matter to the stability of the NPs? In order to answer this question, experiments with a model protein, bovine serum albumin (BSA) in (a) native and (b) completely disordered state were carried out. Initially, the increase in BSA concentration (50–250  $\mu\text{g/mL}$ ) against 1 mM  $\text{AuCl}_3$  showed corresponding increase in Au NP formation as monitored by SPR absorbance (Fig. S11). The

optimum concentration of BSA was 250  $\mu\text{g/mL}$  (3.76  $\mu\text{M}$ ) which produced Au NPs ( $\lambda_{\text{max}}$  531 nm) whereas heat-denatured BSA (3.76  $\mu\text{M}$ ) produced larger Au NPs ( $\lambda_{\text{max}}$  539 nm) (Fig. S12). This suggests that BSA in the denatured state does not effectively stabilize the reduced gold species leading to coalescence and particle aggregates. The reaction of heat-treated cell-free extract (HT-CFE) with native BSA yields smaller size nanoparticles as evidenced by the SPR blue shift of 8 nm which reinforces the importance of protein structure during the formation of nanoparticles (Table 1 and Fig. 5). Investigations on the kinetic studies of the formation of Au NPs with CFE and HTCFE revealed that the rates of nucleation of gold atoms in both the cases differ. Fast nucleation occurs with native CFE (the increase in absorbance from 6 to 12 h

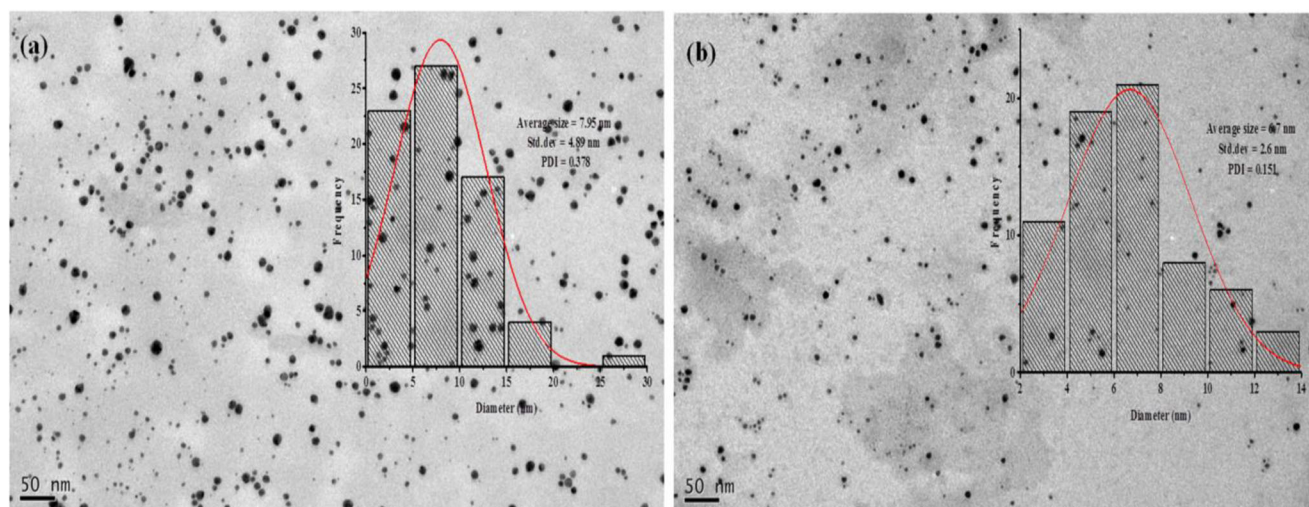
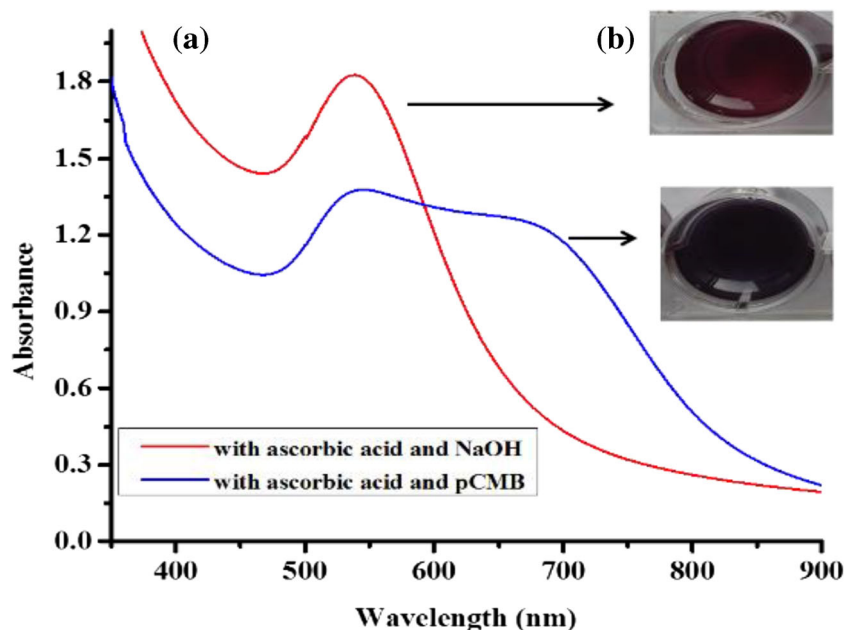


**Fig. 8** Transmission electron micrographs (28,000X) of the gold nanoparticles synthesized using > 3 kDa fraction of cell-free extract in the presence of a NaOH and b pCMB. Inset particle size distribution

**Fig. 9** Synthesis of gold nanoparticles using thiol-modified protein extract of cell-free extract and ascorbic acid as the reducing agent. **a** UV/Vis spectra and **b** visual inspection



with respect to time is  $0.0069 \text{ h}^{-1}$ ) leading to the formation of small nanoparticles of size  $\sim 45 \text{ nm}$  whereas large particles  $\sim 93 \text{ nm}$  were formed with HTCFE (slow nucleation— $0.0036 \text{ h}^{-1}$ ) (Fig. 6). Nucleation of the gold atoms obtained after the reduction of gold (III) ions seem to be influenced by the protein compactness, which imparts stability during Au NP formation.

### 3.4 Effect of Free Protein Thiols in Biosynthesis of Au NPs

Proteins are built up of amino acids which bind to gold atoms and contribute to stabilization of nanoparticles. Hard soft acid base (HSAB) theory postulates that gold interacts with soft

ligands [40] such as sulfhydryl groups. Gold -thiol chemistry is well established and thiol-based ligands such as alkane thiols are reportedly used for the chemical synthesis of monodispersed Au NPs [41]. The effect of one such thiol moiety, cysteine ( $5\text{--}100 \mu\text{M}$ ), was examined for the stability of chemically synthesized Au NPs (Section 2.6). Increased aggregation of Au NPs was observed at  $\geq 10 \mu\text{M}$  cysteine which is represented by secondary  $\lambda_{\text{max}}$  at  $600\text{--}700 \text{ nm}$  and these results are also consistent with TEM analysis (Figs. S13 and S14).

To investigate the role of free protein thiol groups in the synthesis of Au NPs, the thiol groups in the protein extract were derivatized using *p*-chloromercuribenzoic acid (pCMB). Reaction with thiol-modified protein extracts yielded nearly

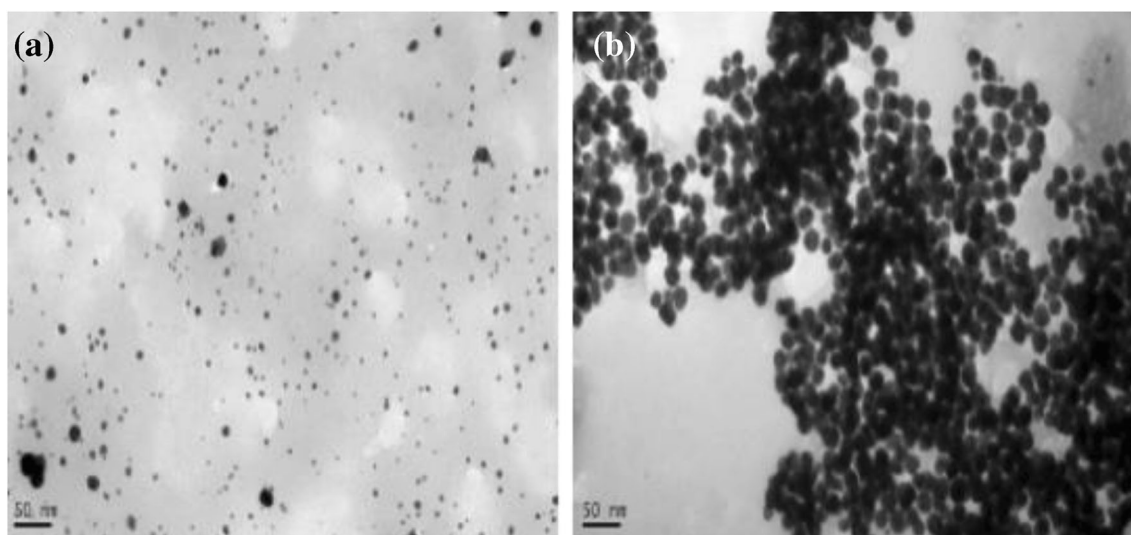


**Fig. 10** Transmission electron microscopy studies of the gold nanoparticles synthesized using thiol-modified protein extract in the presence of ascorbic acid as a reducing agent. **a** NaOH control and **b** thiol-modified extracts



monodisperse Au NPs (Fig. 7) (particle size:  $6.7 \pm 2.6$  nm, polydispersity index (PDI): 0.151) as compared to the nanoparticles produced using native protein extract (particle size:  $7.95 \pm 4.89$  nm, PDI: 0.378) (Fig. 8). Also, the isolated yield of the nanoparticles was low in thiol-modified extracts, i.e., decreased to 56% of that of native protein extract. Interestingly, the synthesis of Au NPs using ascorbic acid (0.2 mM) and thiol-modified protein extract yielded gold aggregates represented by secondary  $\lambda_{\max}$  ( $\sim 600$ – $700$  nm) from UV/Vis spectra (Fig. 9). These results are also consistent with TEM analysis (Fig. 10). Formation of gold aggregates in thiol-modified protein extracts could be due to the lack of sulfhydryl groups. For the reaction with protein extracts in the presence of ascorbic acid, colloidal Au NPs were formed with a characteristic SPR peak around 550 nm ( $\sim 80$  nm). Overall, this study implies that free thiol ( $-\text{SH}$ ) groups control the size of the Au NPs and their polydispersity. In a separate study, the modification of protein thiol inhibits the formation of silver nanoparticles in the cell-free filtrate of *Penicillium nalgiovense* AJ12 [42]. Also, modification of thiol groups in enzymes such as  $\alpha$ -amylase, EcoR1, lactase, and urease inhibits formation of Au NPs [30].

## 4 Conclusions

Systematic studies revealed that the bioreduction of gold (III) ions using the cell-free extract of *Candida parapsilosis* ATCC 7330 is not purely enzymatic; it likely undergoes non-specific reduction utilizing reducing equivalents present within the cell. The native conformation of the protein is crucial for producing stable gold nanoparticles. This was demonstrated using a model globular protein, bovine serum albumin. Free thiol groups in protein extracts leads to formation of polydisperse gold nanoparticles which was controlled by modifying the sulfhydryl group. This strategy can be adapted to produce monodisperse gold nanoparticles in cell-derived extracts. Collectively, this study shows the complexity of yeast-mediated Au NP formation in that the reduction of gold (III) to gold (0) is not specific to reductase enzymes, stabilization occurs with proteins in their original 3D conformation, and free exposed thiol groups of proteins influences the dispersity of gold nanoparticles formed.

**Supplementary Information** The online version contains supplementary material available at <https://doi.org/10.1007/s12668-021-00825-6>.

**Acknowledgments** SK extends his thanks to the Indian Institute of Technology Madras for the HTRA-fellowship. The authors thank the DST-FIST facility of the Department of Biotechnology, Central TEM facility, Sophisticated Analytical Instrumental Facility (SAIF) of IIT Madras.

**Funding** This research was funded by the Board of Research in Nuclear Sciences, Department of Atomic Energy, Government of India (34/14/40/2014-BRNS).

## Compliance with Ethical Standards

**Conflict of interest** The authors declare that they have no conflicts of interest.

**Research Involving Humans and Animals Statement** This research did not involve the use of humans and animals.

**Informed Consent** None.

## References

- Duan, H., Wang, D., & Li, Y. (2015). Green chemistry for nanoparticle synthesis. *Chemical Society Reviews*, 44(16), 5778–5792.
- Dahl, J. A., Maddux, B. L., & Hutchison, J. E. (2007). Toward greener nanosynthesis. *Chemical Reviews*, 107(6), 2228–2269.
- Maliszewska, I. (2011). Microbial synthesis of metal nanoparticles. *Metal Nanoparticles in Microbiology* (pp. 153–175). Berlin, Heidelberg: Springer.
- Korbekandi, H., Irvani, S., & Abbasi, S. (2009). Production of nanoparticles using organisms. *Critical Reviews in Biotechnology*, 29(4), 279–306.
- Anahid, S., Yaghmaei, S., & Ghobadinejad, Z. (2011). Heavy metal tolerance of fungi. *Scientia Iranica*, 18(3), 502–508.
- Yadav, A., Kon, K., Kratosova, G., Duran, N., Ingle, A. P., & Rai, M. (2015). Fungi as an efficient mycosystem for the synthesis of metal nanoparticles: progress and key aspects of research. *Biotechnology Letters*, 37(11), 2099–2120.
- Khandel, P., & Shahi, S. K. (2018). Mycogenic nanoparticles and their bio-prospective applications: current status and future challenges. *Journal of Nanostructure in Chemistry*, 8(4), 369–391.
- Castro, M. E., Cottet, L., & Castillo, A. (2014). Biosynthesis of gold nanoparticles by extracellular molecules produced by the phytopathogenic fungus *Botrytis cinerea*. *Materials Letters*, 115, 42–44.
- Pimprikar, P. S., Joshi, S. S., Kumar, A. R., Zinjarde, S. S., & Kulkarni, S. K. (2009). Influence of biomass and gold salt concentration on nanoparticle synthesis by the tropical marine yeast *Yarrowia lipolytica* NCIM 3589. *Colloids and Surfaces B: Biointerfaces*, 74(1), 309–316.
- Arumugam, P., & Berchmans, S. (2011). Synthesis of gold nanoparticles: an ecofriendly approach using *Hansenula anomala*. *ACS Applied Materials & Interfaces*, 3(5), 1418–1425.
- Mishra, A., Tripathy, S. K., & Yun, S. I. (2011). Bio-synthesis of gold and silver nanoparticles from *Candida guilliermondii* and their antimicrobial effect against pathogenic bacteria. *Journal of Nanoscience and Nanotechnology*, 11(1), 243–248.
- Chauhan, A., Zubair, S., Tufail, S., Sherwani, A., Sajid, M., Raman, S. C., Azam, A., & Owais, M. (2011). Fungus-mediated biological synthesis of gold nanoparticles: potential in detection of liver cancer. *International Journal of Nanomedicine*, 6, 2305.
- Mishra, A., Tripathy, S. K., & Yun, S. I. (2012). Fungus mediated synthesis of gold nanoparticles and their conjugation with genomic DNA isolated from *Escherichia coli* and *Staphylococcus aureus*. *Process Biochemistry*, 47(5), 701–711.
- Kitching, M., Ramani, M., & Marsili, E. (2015). Fungal biosynthesis of gold nanoparticles: mechanism and scale up. *Microbial Biotechnology*, 8(6), 904–917.
- Das, S. K., Das, A. R., & Guha, A. K. (2009). Gold nanoparticles: microbial synthesis and application in water hygiene management. *Langmuir*, 25(14), 8192–8199.

16. Chadha, A., Venkataraman, S., Preetha, R., & Padhi, S. K. (2016). *Candida parapsilosis*: A versatile biocatalyst for organic oxidation-reduction reactions. *Bioorganic Chemistry*, *68*, 187–213.
17. Krishnan, S., Narayan, S., & Chadha, A. (2016). Whole resting cells vs. cell free extracts of *Candida parapsilosis* ATCC 7330 for the synthesis of gold nanoparticles. *AMB Express*, *6*(1), 92.
18. Lin, M. Y., & Yen, C. L. (1999). Antioxidative ability of lactic acid bacteria. *Journal of Agricultural and Food Chemistry*, *47*(4), 1460–1466.
19. Grabar, K. C., Freeman, R. G., Hommer, M. B., & Natan, M. J. (1995). Preparation and characterization of Au colloid monolayers. *Analytical Chemistry*, *67*(4), 735–743.
20. Sedlak, J., & Lindsay, R. H. (1968). Estimation of total, protein-bound, and nonprotein sulfhydryl groups in tissue with Ellman's reagent. *Analytical Biochemistry*, *25*, 192–205.
21. Durán, N., Marcato, P. D., Durán, M., Yadav, A., Gade, A., & Rai, M. (2011). Mechanistic aspects in the biogenic synthesis of extracellular metal nanoparticles by peptides, bacteria, fungi, and plants. *Applied Microbiology and Biotechnology*, *90*(5), 1609–1624.
22. Singh, P., Kim, Y. J., Zhang, D., & Yang, D. C. (2016). Biological synthesis of nanoparticles from plants and microorganisms. *Trends in Biotechnology*, *34*(7), 588–599.
23. Siddiqi, K. S., & Husen, A. (2016). Fabrication of metal nanoparticles from fungi and metal salts: scope and application. *Nanoscale Research Letters*, *11*(1), 98.
24. Boroumand Moghaddam, A., Namvar, F., Moniri, M., Azizi, S., & Mohamad, R. (2015). Nanoparticles biosynthesized by fungi and yeast: a review of their preparation, properties, and medical applications. *Molecules*, *20*(9), 16540–16565.
25. Owaid, M. N., & Ibraheem, I. J. (2017). Mycosynthesis of nanoparticles using edible and medicinal mushrooms. *European Journal of Nanomedicine*, *9*(1), 5–23.
26. Das, S. K., Dickinson, C., Lafir, F., Brougham, D. F., & Marsili, E. (2012). Synthesis, characterization and catalytic activity of gold nanoparticles biosynthesized with *Rhizopus oryzae* protein extract. *Green Chemistry*, *14*(5), 1322–1334.
27. Oyaizu, M. (1986). Studies on products of browning reaction. *The Japanese Journal of Nutrition and Dietetics*, *44*(6), 307–315.
28. Harris, D. C. (2010). *Quantitative chemical analysis*, 8th edn (p. 103). W.H. New York: W.H. Freeman
29. Yamada, E. A., & Sgarbieri, V. C. (2005). Yeast (*Saccharomyces cerevisiae*) protein concentrate: preparation, chemical composition, and nutritional and functional properties. *Journal of Agricultural and Food Chemistry*, *53*(10), 3931–3936.
30. Durán, M., Silveira, C. P., & Durán, N. (2015). Catalytic role of traditional enzymes for biosynthesis of biogenic metallic nanoparticles: a mini-review. *IET Nanobiotechnology*, *9*(5), 314–323.
31. Binupriya, A. R., Sathishkumar, M., Vijayaraghavan, K., & Yun, S. I. (2010). Bioreduction of trivalent aurum to nano-crystalline gold particles by active and inactive cells and cell-free extract of *Aspergillus oryzae* var. *viridis*. *Journal of Hazardous Materials*, *177*(1–3), 539–545.
32. Pfeiffer, C., Rehbock, C., Hühn, D., Carrillo-Carrion, C., de Aberasturi, D. J., Merk, V., Barcikowski, S., & Parak, W. J. (2014). Interaction of colloidal nanoparticles with their local environment: the (ionic) nanoenvironment around nanoparticles is different from bulk and determines the physico-chemical properties of the nanoparticles. *Journal of the Royal Society Interface*, *11*(96), 20130931.
33. Moore, T. L., Rodriguez-Lorenzo, L., Hirsch, V., Balog, S., Urban, D., Jud, C., Rothen-Rutishauser, B., Lattuada, M., & Petri-Fink, A. (2015). Nanoparticle colloidal stability in cell culture media and impact on cellular interactions. *Chemical Society Reviews*, *44*(17), 6287–6305.
34. Li, J., Li, Q., Ma, X., Tian, B., Li, T., Yu, J., Dai, S., Weng, Y., & Hua, Y. (2016). Biosynthesis of gold nanoparticles by the extreme bacterium *Deinococcus radiodurans* and an evaluation of their antibacterial properties. *International Journal of Nanomedicine*, *11*, 5931.
35. Xin, J. Y., Lin, K., Wang, Y., & Xia, C. G. (2014). Methanobactin-mediated synthesis of gold nanoparticles supported over Al<sub>2</sub>O<sub>3</sub> toward an efficient catalyst for glucose oxidation. *International Journal of Molecular Sciences*, *15*(12), 21603–21620.
36. Naraginti, S., & Li, Y. (2017). Preliminary investigation of catalytic, antioxidant, anticancer and bactericidal activity of green synthesized silver and gold nanoparticles using *Actinidia deliciosa*. *Journal of Photochemistry and Photobiology B: Biology*, *170*, 225–234.
37. Sylvestre, J. P., Poulin, S., Kabashin, A. V., Sacher, E., Meunier, M., & Luong, J. H. (2004). Surface chemistry of gold nanoparticles produced by laser ablation in aqueous media. *The Journal of Physical Chemistry B*, *108*(43), 16864–16869.
38. Vroman, L., Adams, A. L., Fischer, G. C., & Munoz, P. C. (1980). Interaction of high molecular weight kininogen, factor XII, and fibrinogen in plasma at interfaces. *Blood*, *55*(1), 156–159.
39. Lemire, J. A., Harrison, J. J., & Turner, R. J. (2013). Antimicrobial activity of metals: mechanisms, molecular targets and applications. *Nature Reviews Microbiology*, *11*(6), 371.
40. LoPachin, R. M., Gavin, T., DeCaprio, A., & Barber, D. S. (2011). Application of the hard and soft, acids and bases (HSAB) theory to toxicant–target interactions. *Chemical Research in Toxicology*, *25*(2), 239–251.
41. Frenkel, A. I., Nemzer, S., Pister, I., Soussan, L., Harris, T., Sun, Y., & Rafailovich, M. H. (2005). Size-controlled synthesis and characterization of thiol-stabilized gold nanoparticles. *The Journal of Chemical Physics*, *123*(18), 184701.
42. Maliszewska, I., Juraszek, A., & Bielska, K. (2014). Green synthesis and characterization of silver nanoparticles using ascomycota fungi *Penicillium nalgiovense* AJ12. *Journal of Cluster Science*, *25*(4), 989–1004.

**Publisher's Note** Springer Nature remains neutral with regard to jurisdictional claims in published maps and institutional affiliations.